HSW VOID AS THE ORIGIN OF COLD SPOT

Anut Sangka[1,2]*, Utane Sawangwit[2], Nuanwan Sanguansak[1], and Teeraparb Chantavat[3]

Received: September 09, 2016; Revised: November 28, 2016; Accepted: December 01, 2016

Abstract

The cosmic microwave background (CMB) cold spot (CS) anomaly is one of the most important unresolved issues in CMB observations. The CS has an angular radius in the sky greater than 5° and a temperature at the centre of about 160 μK which is lower than the average (8.3 times the root mean square of CMB fluctuations). This research is aimed at investigating the origin of the CS as the secondary anisotropy CMB fluctuations, specifically the integrated Sachs-Wolfe (ISW) effect by cosmic voids. The Hamaus, Sutter, and Wendelt void profile is used in the ISW calculation. The calculation shows that the radius of void r_v, the central density contrast δ_c, and the redshift z are needed to be $\mathbf{190^{+30}_{-20}}$Mpc h^{-1}, −0.5 (specific value), and $\mathbf{0.45^{+0.60}_{-0.13}}$, respectively. The void profile can fit the data quite well except for the positive fluctuation region in the CS and the probability of finding such a void is only 10^{-17}.

Keywords: CMB, cosmic voids, ISW effect

Introduction

The cosmic microwave background (CMB) radiation is the earliest electromagnetic signal of the Universe that can be observed. In hot Big Bang cosmology, the CMB is an electromagnetic wave that freely traversed the Universe after the epoch of recombination. The CMB has a black-body spectrum with the current average temperature of 2.725 K. Theoretically, the primordial CMB map is almost smooth everywhere across the Universe with very small Gaussian fluctuations. The root mean square (RMS) of the fluctuations is about 18 μK (Planck Collaboration, 2014). The CMB measurement by Planck has shown that its results almost agree with the standard cosmological model's Lambda cold dark matter (ΛCDM) predictions except for some strange imprinted parts in the CMB map such as the CS. In 2005, Cruz *et al*. analysed the 5-year data of the Wilkinson Microwave

[1] *School of Physics, Institute of Science, Suranaree University of Technology, Nakhon Ratchasima, 30000, Thailand. Tel. 0-4422-4319; Fax. 0-4422-4651; E-mail: m5610396@g.sut.ac.th*

[2] *National Astronomical Research Institute of Thailand, Chiang Mai, 50200, Thailand.*

[3] *The Institute for Fundamental Study, Naresuan University, Phitsanulok, 65000, Thailand.*

[*] *Corresponding author*

Anisotropy Probe (WMAP) mission and found the CS. This large CS is located in the Southern Galactic Cap, $l \approx 209^{o}$, $b \approx -57^{o}$. It has an angular radius about 10^{o} in the sky. The temperature of the centre of the CS is 160 μK lower than the average CMB temperature (8.9 times the RMS). Since, both the temperature and size of the CS deviate from the theoretical prediction significantly, the origin of the CS is not expected to be the primordial CMB anisotropy temperature fluctuations. Other studies such as Finelli *et al*. (2015) and Inoue (2012) point out that the origin of the CS could be the ISW effect due to a super-void. The other explanations are the parallel Universe and the cosmic texture, a remnant of a phase transition in the early Universe (Cruz *et al*., 2007). The ISW effect (Sachs and Wolfe, 1967), is the effect that the photon changes the temperature when it travels though the dynamical gravitational field. In a flat Friedmann-Lemaître-Robertson-Walker (FLRW) universe, the ISW effect occurs if, and only if, the Universe expands; however, it is very sensitive to dark energy. This makes the ISW effect an excellent probe for the dark energy. When a photon travels through dense regions (galaxy clusters), it gains energy and when it comes out it loses energy. But due to the accelerated expansion of the Universe, the galaxy cluster loses its density; the amount of energy that the photon loses when it comes out is less than the amount of energy that is gains when it goes in and, consequently, the temperature of the photon will be increased. On the other hand, when a photon travels through the under-dense regions (voids) it will be colder. For a decelerated universe the results of the ISW effect will be inverse. There are many void profiles, which were proposed to solve the origin of the CS. Most of those models prefer the radius of the void ($r_{\rm v}$) to be greater than 150 Mpc h^{-1}. For example, Finelli *et al*. (2015) uses the Λ-Lemaître-Tolman-Bondi (LTB) geometry to find the density perturbation of a void. This work states that the super-void has a radius $r_{\rm v} = 190^{+39}_{-27}$ Mpc h^{-1}, with the central density contrast $\delta_{\rm c} = 0.37^{+0.22}_{-0.12}$. That void should be located at redshift $z_0 = 0.15^{+0.04}_{-0.05}$. In 2014, Hamaus, Sutter, and Wendelt (HSW) proposed the universal void density profile in Hamaus *et al*. (2014). The HSW profile was obtained from N-body simulations. This profile can fit the observational data very well, especially for the voids of a radius $10 < r_{\rm v} < 60$ Mpc h^{-1} (Hamaus *et al*., 2014). For the voids with a radius greater than 60 Mpc h^{-1} the profile is not well examined due to the lack of data in the simulations. In this work, we try to extrapolate the HSW profile to a high radius and try to fit the ISW effect of the HSW profile to the CS.

Theoretical Background

HSW Void Profile

The HSW void density profile has 3 parameters, the central density contrast $\delta_{\rm c}$, the radius $r_{\rm v}$, and the scale radius $r_{\rm s}$ at which the density contrast is zero.

$$\delta(r) = \frac{\rho_V}{\bar{\rho}} - 1 = \delta_{\rm C}\frac{1-(r/r_{\rm S})^{\alpha}}{1+(r/r_V)^{\beta}}, \quad (1)$$

where ρ_V and $\bar{\rho}$ are the density of the void and mean cosmic density, respectively. α and β have an approximately linear relation with $r_{\rm S}/r_{\rm V}$ by the following equations:

$$\alpha(r_{\rm S}/r_{\rm V}) \simeq -2(r_{\rm S}/r_{\rm V} - 2), \quad (2)$$

$$\beta \simeq \begin{cases} 17.5\, r_s/r_V - 6.5 & \text{for } r_s/r_V < 0.91 \\ -9.8\, r_s/r_V + 18.6 & \text{for } r_s/r_V \geq 0.91 \end{cases} \quad (3)$$

We can write Equation (1) as a function of $x = r/r_{\rm v}$,

$$\delta(r) = \frac{\rho_V}{\bar{\rho}} - 1 = \delta_{\rm C}\frac{(1-\lambda x^{\alpha})}{(1+x^{\beta})}, \quad (4)$$

where $\lambda = (r_s/r_{\rm v})^{-\alpha}$. The plot between the profile of Equation (1) and observational data is illustrated in Figure 1. One of the special features of the HSW profile is that it includes a positive density contrast region (a so-called void compensation) (Hamaus *et al*., 2014), while other void density profiles do not include this. Figure 1 shows that the HSW profile can describe the void compensation well.

ISW Effect Calculation

The ISW temperature fluctuation $\Delta T_{\rm ISW}(\hat{n})$ at the direction $\hat{n}$ can be calculated by

$$\frac{\Delta T_{\mathrm{ISW}}(\hat{n})}{\bar{T}} = -\frac{2}{c^2}\int_0^{z_{\mathrm{LS}}} \frac{\partial \Phi(z,\hat{n})}{\partial z} dz \qquad (5)$$

where the integration is performed from the redshift $z = 0$ to the last scattering surface $z_{\mathrm{LS}} \approx 1000$. The Newtonian potential Φ relates to the density contrast δ by the Poisson equation,

$$\nabla^2\Phi = 4\pi G a^2 \bar{\rho} D_+(z)\delta(z=0), \qquad (6)$$

where G is the Newton universal gravitation constant, a is scale factor ($a = 1/(1+z)$), and $D_+(z)$ is the linear growth factor.

Equation (5) can be discretised to the summation form by,

$$\int_0^{z_{\mathrm{LS}}} \frac{\partial \Phi(z,\hat{n})}{\partial z} dz \rightarrow \sum_i \{\Phi(z_{i+1},\hat{n}) - \Phi(z_{i-1},\hat{n})\}. \qquad (7)$$

With linear perturbation density, the summation can be described by

$$\sum_i \{\Phi(z_{i+1},\hat{n}) - \Phi(z_{i-1},\hat{n})\} = \sum_i D_+(z_i)\{\Phi_0(D_d(z_{i+1}),\hat{n}) - \Phi_0(D_d(z_{i-1}),\hat{n})\}, \qquad (8)$$

where $\Phi_0(D_d(z),\hat{n})$ is the non-redshift evolution Newtonian potential at the angular diameter distance $D_d(z)$ in the direction $\hat{n}$.

CMB Weak Gravitational Lensing

On a small scale (<1°) the weak gravitational lensing effect can change the appearance of the CMB map by deflecting the photon's trajectory with the deflection angle $\hat{\alpha}$. Regarding the lensed CMB temperature anisotropy in the direction $\hat{n}$ in the sky, $\tilde{T}(\hat{n})$ is equivalent to an unlensed anisotropy $T(\hat{n} + \hat{\alpha})$. Because the deflection angle $\hat{\alpha}$ is very small, we can use Taylor's expansion to approximate $\tilde{T}(\hat{n})$ as

$$\tilde{T}(\hat{n}) = T(\hat{n}) + \alpha_i \partial^i T(\hat{n}) + \frac{1}{2}\alpha_i\alpha_j\partial^i\partial^j T(\hat{n}) + \mathcal{O}(\alpha^3). \qquad (9)$$

The deflection angle $\hat{\alpha}$ for a typical void ($15 \leq r_V \leq 30$ Mpc h^{-1} and $r_S/r_{\mathrm{V}} \simeq 0.91$) can be calculated by finding the gradient of lensing potential $\psi(\theta)$,

$$\hat{\alpha}(\theta) = \nabla_\theta \psi(\theta) \qquad (10)$$

The lensing potential is defined by

$$\psi(\theta) = -\frac{2}{c^2}\int \Phi(\chi,\hat{n}) d\chi \qquad (11)$$

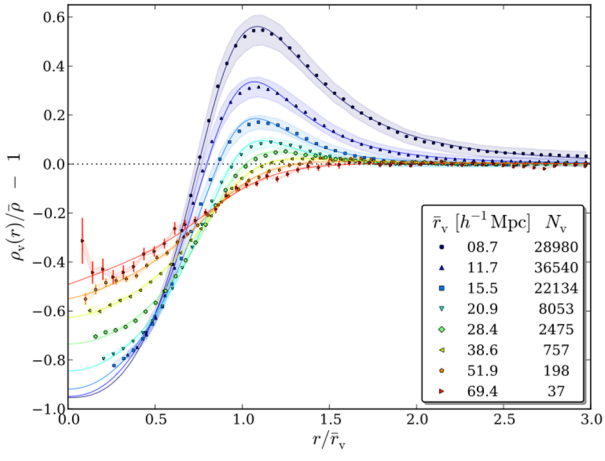

Figure 1. Stacked density profiles of voids at redshift zero in 8 sets of the voids' radii. The shaded regions represent the standard deviation σ of each stacks (scaled down by 20 forvisibility), while the error bars come from standard errors on the mean profile $\sigma/\sqrt{N_V}$ where N_V is the number of voids. The solid lines are the best fit solutions from the density profile of Equation (1). The picture is captured from Hamaus *et al.*, (2014)

where we integrate along the line of sight χ. For the HSW void profile with $r_s/r_v = 0.91$, Chantavat *et al*. (2016) show that the lensing potential can be described by

$$\psi(b/r_V, r_V, z) \simeq S(r_V, z) \times \tilde{\psi}(b/r_V), \qquad (12)$$

where the impact parameter $b = D_d\theta$, D_d is the angular diameter distance to the lens plane, $\tilde{\psi}(x)$ is the scale-invariant lensing potential, and $S(r_V, z)$ is the lensing potential scaling factor.

$$\tilde{\psi}(x) = \psi_0 \exp(\Gamma_0 x^{\gamma_0}) \times (1.0 + x^{\gamma_1})^{\gamma_2}, \qquad (13)$$

where

$\psi_0 = 9.06 \times 10^{-2}$ Mpc^2 h^{-2},
$\gamma_0 = 1.29$,
$\gamma_1 = 2.86$,
$\gamma_2 = -1.72$, and
$\Gamma_0 = -0.31$.

$$S(r_V, z) = \frac{16\pi G}{c^2}\Omega_m \rho_{\text{cri}} \left(\frac{r_V}{\text{Mpc}\, h^{-1}}\right)^3 \frac{(1+z)^3 D_+(z)}{(D_d/\ \text{Mpc}\, h^{-1})}, \qquad (14)$$

where Ω_m is the density parameter of matter and ρ_{cri} is the critical density.

Result and Discussion

ISW and CMB Weak Lensing Comparison

As mentioned earlier, the ISW effect is a large-scale effect. In contrast, the weak gravitational lensing, which only changes the appearance of the CMB map, is a small-scale effect. For example, if we consider a typical void of size $10 < r_v < 45$ Mpc h^{-1} and find the ISW effect and CMB weak lensing of such a void, we will see that the contribution of the ISW effect is dominant (Figure 2). Consequently, the contribution from the weak lensing effect can be ignored for the CS temperature.

Measure the CS One Dimensional Temperature Profile

The Planck SMICA 2015 data has been used in this research. We obtain the 1-dimensional CS temperature profile by finding the average temperature fluctuations within a ring, where each ring has a thickness of 1°. For example, the average temperature at θ 1.5° ($\Delta T(\theta = 1.5°)$) is

$$\Delta T(\theta = 1.5°) = \frac{1}{N}\sum_{1°<\theta<2°} \Delta T(\theta) \qquad (15)$$

where N is the number of pixels inside the ring with an inner radius of 1° and an outer radius of 2° and we sum over all pixels inside the ring. The uncertainty of the CS profile at data point i (σ_i) is calculated by random generation of 1000 CMB maps and calculating the standard deviation inside the rings over the 1000 maps.

Cold Spot Fitting Data

In order to test the model, the χ^2_{reduced} method is used to find a goodness of fit. We describe only a summary of this method; for more details the readers can follow Press *et al*. (2007). Let ΔT_i^{obs} be the observed temperature at the data point ith, ΔT_i^{ISW} be the ISW

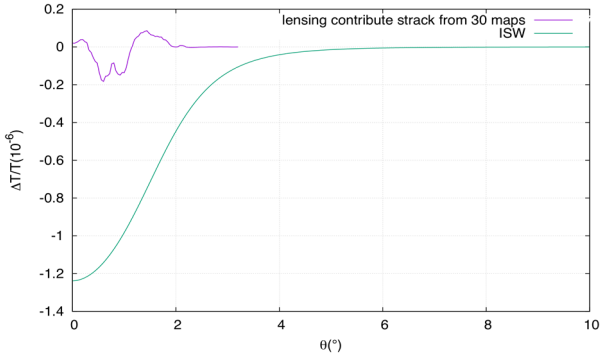

Figure 2. A comparison between the ISW and CMB weak lensing effects for a void of radius $r_V = 30$ Mpc h^{-1}; it is obvious that the ISW is dominant

temperature at data point ith, and σ_i be the uncertainty of observational data at data point ith, then the χ^2 will be

$$\chi^2 = \sum_i \frac{\left(\Delta T_i^{\mathrm{ISW}} - \Delta T_i^{\mathrm{obs}}\right)^2}{\sigma_i^2} \qquad (16)$$

The $\chi^2_{\mathrm{reduced}}$ is just χ^2 divided by the number of degrees of freedom, which is the number of data points subtracted by the number of free parameters.

$$\chi^2_{\mathrm{reduced}} = \frac{\chi^2}{\text{degrees of freedom}} \qquad (17)$$

In this research the number of data points is 30 (we have 30 θ positions) and 4 parameters (δ_{C}, z, r_V and r_S/r_V). Hence, the number of degrees of freedom is 26. The parameter set that gives us the minimum χ^2 is the best-fit parameter set. We also report the $\chi^2_{\mathrm{reduced}}$ calculated from the minimum χ^2 using Equation (17). The $\chi^2_{\mathrm{reduced}}$ can be used to indicate the goodness of fit of the model. If it is close to 1, then the model is considered to be a good fit. For $\chi^2_{\mathrm{reduced}}$ that is much greater than 1, it indicates that the model is not good enough, while a value much lower than 1 means that the measured uncertainty could be over-estimated.

Figure 3 shows the ISW effect from the best-fit parameter set fit to the CS temperature profile. The void parameters are $z = 0.45$, $\delta_c = 0.5$, $r_{\mathrm{v}} = 190$ Mpc h^{-1}, $r_{\mathrm{s}}/r_{\mathrm{v}} = 0.91$, and $\chi^2_{\mathrm{reduced}} = 0.99$ (with degrees of freedom 26). We can see that the ISW effect approaches zero from the negative while the region near the edge of the CS ($r \approx 15^{\mathrm{o}}$) has the positive fluctuations. Figure 4 shows the χ^2 contour plot between parameters. From the plot, we can see that there are correlations between those sets of parameters. In fact, Hamaus *et al.* (2014) shows that δ_c tends to be -0.5 for a void with a radius greater than 70 Mpc h^{-1} and $r_{\mathrm{s}}/r_{\mathrm{v}} = 0.91$ for an effective value. If we follow this assumption, the best fit parameters are now

$$\delta_{\mathrm{C}} = -0.5,$$
$$r_{\mathrm{V}} = 190^{+30}_{-20}[\mathrm{Mpc}\ h^{-1}],$$
$$r_{\mathrm{s}}/r_{\mathrm{v}} = 0.91,$$
$$\chi^2_{\mathrm{reduced}} = 0.99.$$

Comparing to the other void profiles such as Finelli *et al.* (2015), we found that the HSW void also provides a void of radius greater than 150 Mpc h^{-1} to fit the CS. For the positive fluctuation region, which is at the edge of the CS, the fluctuation is much lower than inside the CS. We may assume that this is the ISW effect due to galaxy clusters (the over-dense region, the opposite of the void) or it may be just the normal CMB fluctuation (30 μK is less than 3σ of the CMB temperature fluctuations). Note that, from Hamaus *et al.* (2014), the HSW profile is only well approximated up to $r_{\mathrm{V}} \leq 60$ Mpc h^{-1}. In this work, we extrapolate the profile to a larger size.

In addition, we not only calculate the ISW effect of the HSW void. We also find that the probability of a void with a radius greater than 150 Mpc h^{-1} would exist by considering the void abundance (Pisani *et al.*, 2015),

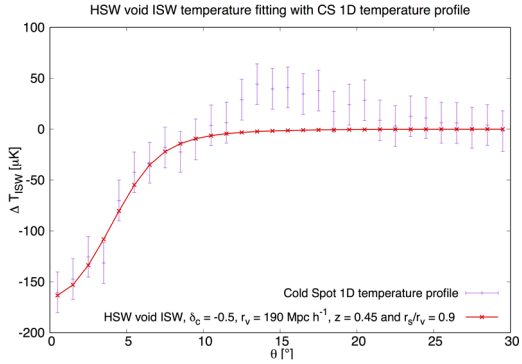

Figure 3. The best-fit parameter set of HSW void ISW to the CS 1-dimensional temperature profile

$$\frac{Mn(M,z)}{\bar{\rho}}\frac{dM}{M} = \nu f(\nu)\frac{d\nu}{\nu}, \quad (18)$$

where M is the void mass, $\bar{\rho}$ the background density, and *n(M, z)* the number density of voids of a given mass and redshift. The fraction $f(\nu)$ of mass that has evolved into voids can be approximated as:

$$\nu f(\nu) \approx \sqrt{\frac{\nu}{2\pi}}\exp(-\nu/2), \quad (19)$$

where $\nu = \delta_v^2/\sigma_M^2(M)$ is the critical under-density of void formation and $\sigma_M^2(M)$ is the variance of linear density fluctuations on a scale $R = \left(\frac{3M}{4\pi\bar{\rho}}\right)^{-1/3}$. The indication from Pisani *et al*. (2015) is that the appropriate value of δ_V is -0.45. By applying Equation (19), we can find the probability that a void of a radius greater than 150 Mpc h^{-1}, is ≈ 10^{-17}. This can be interpreted that the origin of the CS may not be the ISW effect due to a super-void or that the large-scale structure formation theory is incomplete or that the ΛCDM is missing something. Another interpretation is the multiverse cosmology, which predicts that our Universe is just the local Universe and that there would be at least 10^{17} Universes to ensure that the super-void exists.

Conclusions

In this work, we aim to investigate the origin of the CS as the secondary anisotropy CMB fluctuations due to a super-void. Our void model is the HSW void profile, which is claimed to be the universal void profile by Hamaus *et al*. (2014). The calculation of the ISW and the weak lensing effect had shown that the ISW effect is the dominant effect on a large scale. The best-fit parameters of the HSW void are δ_c= -0.5 (specific value), r_V = 190^{+30}_{-20} Mpc h^{-1}, r_s/r_V = 0.91, $z = 0.45^{+0.60}_{-0.13}$, and the goodness of fit χ^2_{reduced}= 0.99 with 26 degrees of freedom. The size of the void is extrapolated from typical voids ($15 \leq r_V \leq 70$ Mpc h^{-1}) to a super-void ($r_V \geq 120$ Mpc h^{-1}). This indicates that the HSW profile could be used to describe large voids. The CS data shows that there is a hot region near the

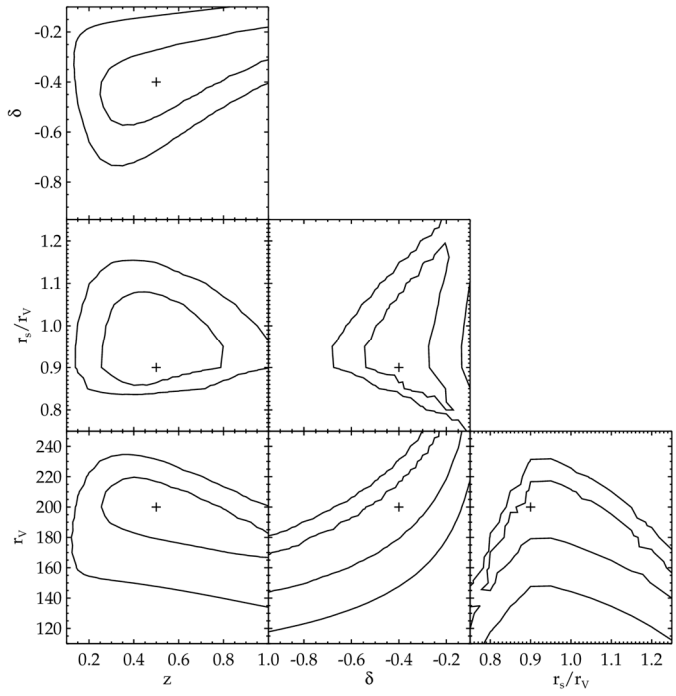

Figure 4. χ^2 contour plot between parameters

edge of the CS, which may be the ISW due to a galaxy cluster or just a normal fluctuation. The probability of a super-void of a size greater than 150 Mpc h^{-1} is extremely low (10^{-17}) which means the origin of the CS is probably not the ISW effect due to a super-void.

Acknowledgements

This work could not have been done if the following did not provide support both in terms of funding and facilities: Suranaree University of Technology (SUT), SUT scholarships for outstanding students, the Thailand Research Fund (TRF) under Grant Number IRG57800010, and Naresuan University provided the funds and opportunity for us to work together; the National Astronomical Research Institute of Thailand provided both funding and allowed us to use its High Performance Computing (HPC) cluster.

References

Chantavat, T., Sawangwit, U., Sutter, P.M., and Wandelt, B.D. (2016). Cosmological parameter constraints from CMB lensing with cosmic voids. Phys. Rev. D, 93(4):043523.

Cruz, M., Martínez-González, E., Vielva, P., and Cayón, L. (2005). Detection of a non-Gaussian spot in WMAP. Mon. Not. R. Astron. Soc., 356:29-40.

Cruz, M., Turok, N., Vielva, P., Martínez-González, E., and Hobson, M. (2007). A cosmic microwave background feature consistent with a cosmic texture. Science, 318:1,612-1,614.

Finelli, F., Garcia-Bellido, J., Kovacs, A., Paci, F., and Szapudi, I. (2015). Supervoids in the WISE-2MASS catalogue imprinting cold spots in the cosmic microwave background. Mon. Not. R. Astron. Soc., 455:1,246-1,256.

Hamaus, N., Sutter, P.M., and Wandelt, B.D. (2014). Universal density profile for cosmic voids. Phys. Rev. Lett., 112(25):251302.

Inoue, K.T. (2012). On the origin of the cold spot. Mon. Not. R. Astron. Soc., 421:2,731-2,736.

Pisani, A., Sutter, P.M., Hamaus, N., Alizadeh, E., Biswas, R., Wandelt, B.D., and Hirata, C.M. (2015). Counting voids to probe dark energy. Phys. Rev. D, 92(8):083531.

Planck Collaboration: Ade, P.A.R., Aghanim, N., Alves, M.I.R., Armitage-Caplan, C., Arnaud, M., Ashdown, M., Atrio-Barandela, F., Aumont, J., Aussel, H., *et al*. (2014). Planck 2013 results. I. Overview of products and scientific results. Astron. Astrophys., 571A1:1-48.

Press, W.H., Teukolsky, S.A., Vetterling, W.T., and Flannery, B.P. (2007). Numerical Recipes: The Art of Scientific Computing. 3rd ed. Cambridge University Press, New York, NY, USA, 1,235p.

Sachs, R.K. and Wolfe, A.M. (1967). Perturbations of a cosmological model and angular variations of the microwave background. Astrophys. J., 147:73-90.